

Nb-Ti Based Alloy Powder Prepared by Hydride-Dehydride Method

Li Qijun^{1,2}, Zhang Lin¹, Li Bingbing¹, Wei Dongbin¹, Qu Xuanhui¹

¹Beijing Advanced Innovation Center for Materials Genome Engineering, Institute for Advanced Materials and Technology, Beijing Laboratory of Metallic Materials and Processing for Modern Transportation, University of Science and Technology Beijing, Beijing 100083, China; ²Aerospace Research Institute of Material and Processing Technology, Beijing 100076, China

Abstract: Micro-fine lightweight Nb-Ti based alloy powder was fabricated by a hydride-dehydride method, and the hydrogen absorption/desorption behavior was investigated. Results show that obvious hydrogen absorption occurs at 300 °C, and the absorbed hydrogen quantity reaches a saturation value of 1.12 wt% at 400 °C. Binary and ternary hydrides ($\text{Nb}_{0.803}\text{V}_{0.197}\text{H}$, $\text{Nb}_{0.696}\text{V}_{0.304}\text{H}$ and TiH_x) are formed after hydrogenation. Hydrogen-induced embrittlement facilitates the pulverization of the thin alloy plate. During dehydrogenation process, hydrogen content is effectively reduced to 0.001 wt% at 300 °C. Phase transformation from niobium or titanium hydrides to single phase solid solution alloy (β phase) is achieved. Oxygen content of the powder increases with increasing hydrogenation or dehydrogenation temperature due to the high reactivity of constituent elements with oxygen, and both hydrogenation and dehydrogenation temperature of 400 °C is selected in order to prevent severe oxygen intake. Micro-fine Nb-based alloy powder with average particle size $< 10 \mu\text{m}$ and oxygen content of 2980 $\mu\text{g/g}$ is obtained. Superficial contamination of the obtained powder is detected, and oxygen impurity exists in the form of Nb_2O_5 and TiO_2 .

Key words: powder metallurgy; Nb-Ti based alloy; powder preparation; hydrogenation; dehydrogenation

With low density, high melting point, high strength, and favorable oxidation resistance, Nb-Ti based alloy has attracted increasing attention as a promising high-performance lightweight refractory metal for high-temperature structural application in aerospace and military weapon industries^[1-3]. A multicomponented, body centered cubic solid solution strengthened Nb-Ti based alloy is developed, aiming at service temperatures above 1200 °C. This temperature is beyond the scope of Ni-based superalloys^[4,5]. The alloying elements not only ensure high temperature strength and oxidation resistance of the alloys but also lower density (6.85 g cm^{-3}). Conventionally, Nb-Ti based alloys were fabricated by vacuum arc melting, casting and rolling^[6-8]. The complexities in their thermo-mechanical processing and the subsequent machining,

coarse microstructure and composition macrosegregation greatly restrict their widespread usage. The complex shaped Nb-Ti based alloy components are difficult to be fabricated due to its high resistance to deformation and hard machinability. In order to overcome these shortcomings, a powder metallurgy based processing approach has attracted increasing attention in recent years as it offers the prospect of producing complex shaped parts with homogeneous microstructure and fine grains.

Raw powder material with fine particle size and low oxygen content is prerequisite for niobium powder metallurgy. The preparation of Nb-Ti based powder has several difficulties due to its high melting temperature and high activity. The traditional powder preparation process of Nb-Ti alloy mainly involves mechanical alloying and atomization

Received date: January 25, 2019

Foundation item: National Natural Science Foundation of China (51574029, 51604240, 51574030); National Key R&D Program of China (2017YFB0305600, 2017YFB0306000)

Corresponding author: Zhang Lin, Ph. D., Professor, Beijing Advanced Innovation Center for Materials Genome Engineering, Institute for Advanced Materials and Technology, University of Science and Technology Beijing, Beijing 100083, P. R. China, Tel: 0086-10-82377286, Fax: 0086-10-62334311, E-mail: zhanglincsu@163.com; quxh@ustb.edu.cn

Copyright © 2020, Northwest Institute for Nonferrous Metal Research. Published by Science Press. All rights reserved.

technologies^[9,10]. Due to the high melting temperature of Nb-Ti alloy, argon atomization (AA) is no longer applicable. Mechanical alloying has the disadvantage of low efficiency and high risk of contamination^[11,12]. Although the spherical powder prepared by plasma rotating electrode process (PREP) is suitable for powder metallurgy route, the low yield rate of fine powder and the high cost restricts its widespread application. It is necessary to develop more effective powder production methods for Nb-based fine powder.

The hydride-dehydride (HDH) process provides a more applicable method for the fabrication of Nb-Ti based alloy powder^[13-15]. The alloy is converted to hydrides by absorbing a significant amount of hydrogen, which facilitates the embrittlement of the alloy. The hydrogenated alloy can be easily pulverized to fine particles. Subsequently, the alloy undergoes vacuum dehydriding by heating in vacuum to obtain the corresponding metal powder. The great advantage of this technique is its low cost and fine particle size compared with other techniques such as atomization or mechanical alloying. Understanding hydrogen absorption and desorption behavior of the alloy is of vital importance for the control of powder properties. Up till now, there are very few reports on the HDH process of Nb-Ti based alloy powder.

The objective of this work is to explore alternative powder production method (HDH) for Nb-Ti based alloy powder, which is beneficial to solve the difficulties in preparation caused by its high melting temperature and high activity. The main parameters of hydrogenation and dehydrogenation process were optimized in order to obtain fine particle size with a controllable oxygen content.

1 Experiment

Table 1 lists chemical composition of the Nb-Ti based alloy. Bulk metals (purity $\geq 99.9\%$) of Nb, Ti, Al, V, Cr, W and Hf were purchased from Cuibailin Nonferrous Metal Development Center (China). The alloy bar was prepared by vacuum arc remelting. The alloy ingot was homogenized at 1200 °C for 5 h in a ZW-15-20 vacuum furnace, and then furnace-cooled to room temperature. The homogenized ingot was cut into thin slices with thickness of 2 mm. The slices were cleaned with acetone. The hydriding experiments were carried out in a tungsten coil furnace at 200~800 °C. Initially, the furnace was evacuated up to 10^{-3} Pa. After reaching the desired temperature, hydrogen gas (99.999% purity) was introduced into the furnace under the pressure of 0.2 MPa, keeping both pressure and temperature constant for 1 h. After hydrogenation, the furnace was cooled in hydrogen to 150 °C at a cooling rate of 1 °C/min. The hydrogenated Nb-Ti based alloy was pulverized by disc refiner in Ar atmosphere, and then sieved into fine particle. The dehydriding process was performed in vacuum furnace

(10^{-3} Pa) at 100~800 °C for 30 min. Differential scanning calorimetry (DSC) analysis was carried out on a STA 409 instrument (Netzsch-Geraetebau GmbH, Bayern, Germany). The microstructure of the ingot and the powder was observed on a JSM-6480LV scanning electron microscope (SEM) equipped with energy-dispersive X-ray spectroscope (EDS). Phase constituents were characterized by a Rigaku D/MAX RB X-ray diffractometer (XRD) using Cu radiation. The hydrogen and oxygen contents of the powders were measured by an inert gas fusion thermal conductivity method according to ASTM E1447-09. The X-ray photoelectron spectrometer (AXIS ULTRADLD) was used to analyze the surface state of the powder particles. Particle size distribution of the powders was measured on a LMS-30 laser particle size analyzer.

2 Results and Discussion

2.1 Nb-based alloy ingot

Homogenizing treatment of the ingot is prerequisite for the fabrication of the powders with uniform element distribution. Fig.1a shows the back scattered electron image of the vacuum arc-remelted ingot. Table 2 lists the result of EDS analysis for the vacuum arc-remelted ingot. Some cavities (the dark spots on Fig.1a) are formed due to solidification contraction. Regions with different contrast are observed, suggesting the existence of local inhomogeneity in composition. The light grey area (A) has a higher content of Nb and a lower content of Ti and Al compared with that of the dark grey area (B).

As for the ingot annealed at 1200 °C for 5 h, the main alloying elements, Nb, Ti and V, exhibit a high composition uniformity, as shown in Fig.1b.

Fig.2 shows the XRD pattern of the homogenized Nb-Ti based alloy. The main phase is Nb-Ti based solid solution (β phase) with a body centered cubic structure, indicating that all the alloying elements are dissolved in the niobium matrix.

2.2 Hydrogenation and pulverization

With the aim to figure out the process in which hydrogen penetrates, hydrogen absorption behavior was investigated, followed by oxygen impurity variations during hydrogenation process due to its pronounced impact on densification behavior and mechanical properties. Fig.3 shows the hydrogen and oxygen contents of the slices hydrogenated in the temperature range of 200~800 °C. When the temperature is lower than 300 °C, the increase in absorbed hydrogen is not obvious, and the hydrogen content is lower than

Table 1 Chemical composition of the Nb-Ti based alloy (wt%)

Nb	Ti	Al	V	Cr	W	Mo	Hf
60.93	21.14	2.80	5.58	4.26	2.64	0.50	2.10

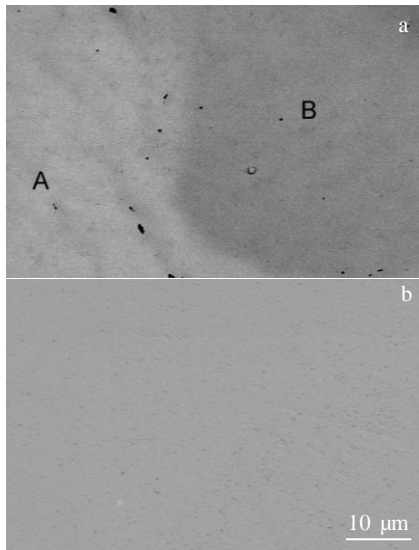


Fig.1 BSE images of the vacuum arc-remelted ingot (a) and the homogenized ingot (b)

Table 2 EDS result of A and B area in the cross section of the powder in Fig.1a (wt%)

Area	Nb	Ti	Al	V	Hf	W	Mo	Cr
A	63.01	19.02	2.54	5.40	2.15	2.39	0.51	4.98
B	40.14	45.72	3.83	6.12	0.84	-	-	3.34

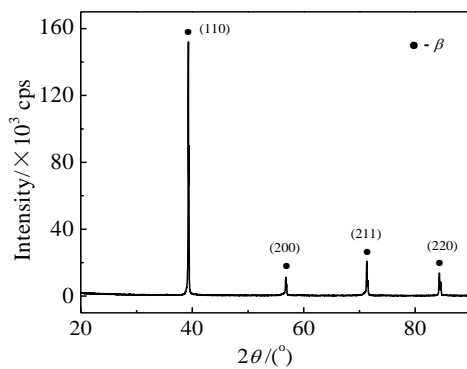


Fig.2 XRD pattern of homogenized Nb-Ti based alloy

0.02 wt%. A sharp increase in the absorbed hydrogen quantity is observed in the temperature range of 300~400 °C. Hydrogen content increases to 1.12 wt% at 400 °C. When the hydrogenation temperature is higher than 400 °C, the adsorbed-hydrogen quantity reaches a stable value, indicating that hydrogen has been saturated in the Nb-Ti based alloy. Although the alloying elements (Nb, Ti and V) in the alloy are all highly reactive to hydrogen, the quantity of the absorbed hydrogen is lower than that of the Ti (4 wt%~5 wt%) and Ti-6Al-4V alloy (3 wt%~4 wt%)^[14]. This is

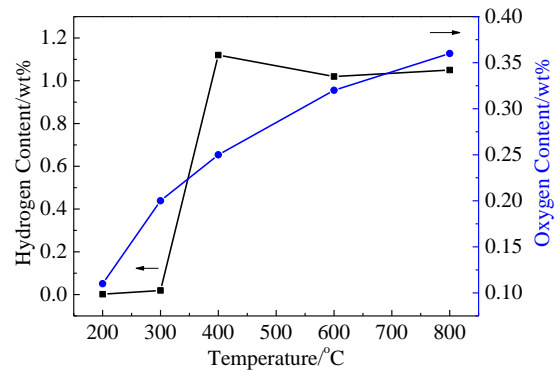


Fig.3 Hydrogen and oxygen contents of the powder hydrogenated at different temperatures

associated with the crystal structure and the degree of ordering^[16]. However, the absorbed hydrogen is enough to facilitate the embrittlement of the plate with the thickness of 2 mm. Oxygen content of the hydrogenated powder increases with increasing hydrogenation temperature due to the high reactivity of constituent elements (such as Nb, Ti, Al, V) with oxygen. On the consideration of the hydrogen embrittlement effect and the oxygen contamination, the most suitable hydrogenation temperature of 400 °C is selected.

Fig.4 shows the XRD patterns of the powder hydrogenated at different temperatures. In the hydrogenation temperature range of 200~800 °C, the relative intensity of $\text{Nb}_{0.803}\text{V}_{0.197}\text{H}$ increases with the increasing temperature, indicating the increased content of absorbed hydrogen and the formation of niobium hydride. At 200 °C, the peaks of β phase vanish and $\text{Nb}_{0.696}\text{V}_{0.304}\text{H}$ phase is formed instead, suggesting that the alloy has a high capability of hydrogen absorption, and that the hydrogenation reaction of the alloy occurs at the temperature as low as 200 °C. A comparison of the peak positions of hydrides of the 200, 400 and 600 °C annealed samples reveals that the peaks move slightly towards lower 2θ values because of the hydrogen-induced expansion of the crystal structure, which is in accordance with the result reported by Oh et al^[17,18]. At 800 °C, significant broadening and intensity reduction of the peaks of $\text{Nb}_{0.803}\text{V}_{0.197}\text{H}$ and TiH_2 hydrides is observed, which is attributed to the fragmentation of brittle hydride. The structural transition of $\text{Nb}_{0.696}\text{V}_{0.304}\text{H}$ hydride to $\text{Nb}_{0.803}\text{V}_{0.197}\text{H}$ and TiH_2 occurs at 800 °C with the increased content of absorbed hydrogen.

The phase purity, surface composition, and chemical states of the hydrogenated powder were further investigated by XPS measurements. Fig.5 shows the XPS spectra of the hydrogenated powder. It is revealed in Fig. 5a that Nb, Ti, V and O are the main elements on surface of the hydrogen-

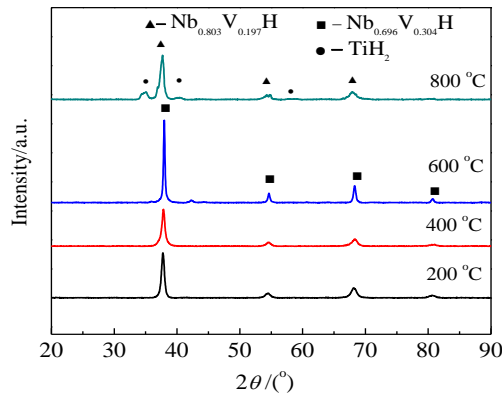


Fig.4 XRD patterns of the powder hydrogenated at different temperatures

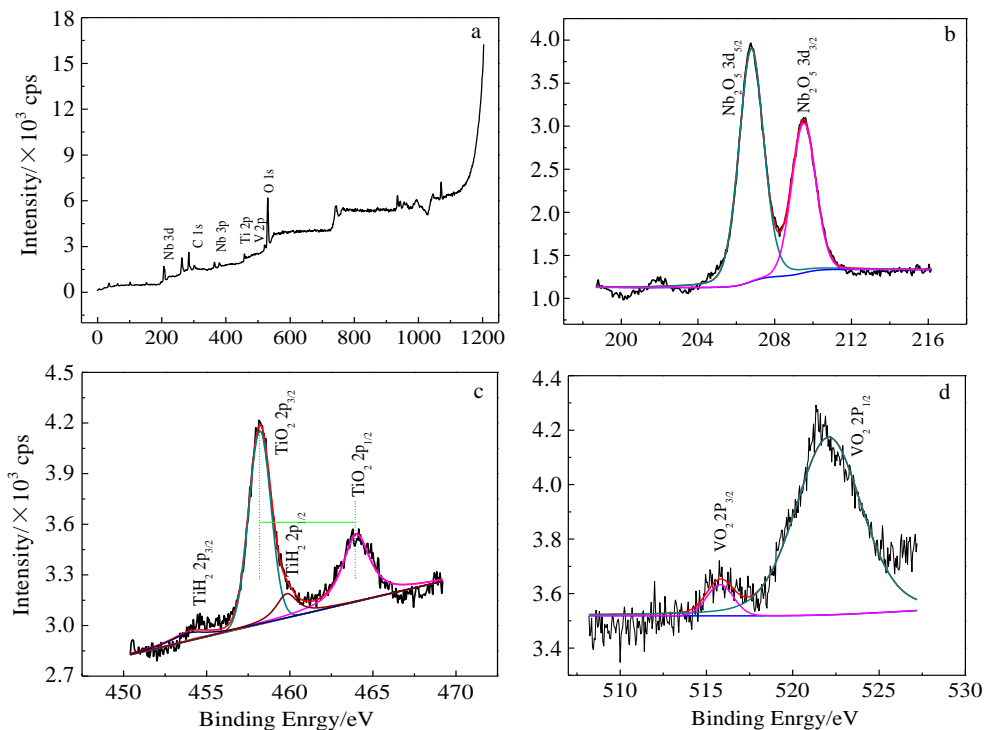


Fig.5 XPS spectra of the hydrogenated powder: (a) full spectrum; (b) Nb 3d, (c) Ti 2p, and (d) V 2p

correspond to the V $2p_{3/2}$ state and the V $2p_{1/2}$ state for standard VO_2 , respectively. The XPS results illustrate that the main compounds on surface of the hydrogenated powder are TiO_2 , Nb_2O_5 and VO_2 .

Fig.6 shows the SEM images of the hydrogenated plates. A lot of cracks and fissures are observed, as marked by the circles. During hydrogenation, interstitially dissolved hydrogen is trapped preferably in areas of local stress concentrations, such as vacancies, dislocations, precipitations, phase and grain boundaries, which cause crystal lattice distortion around hydrides due to the increase of dislocation density^[20,21]. The penetration of hydrogen atoms induces embrittlement effect, which facilitates pulverization of the

hydrogenated powder. The Nb 3d XPS spectrum (Fig.5b) was deconvoluted into two major peaks with a binding energy values of 209.5 and 206.8 eV, corresponding to the Nb $3d_{1/2}$ and Nb $3d_{3/2}$ spin-orbit peaks of the Nb_2O_5 phase, respectively. Fig.5c shows the Ti 2p XPS spectrum. The spectrum was deconvoluted to several Gaussian peaks using a peak synthesis procedure. Two peaks of $2p_{3/2}$ and $2p_{1/2}$ with better symmetry at the peak binding energies of 463.9 and 458.2 eV, corresponds to the 2p binding energy of the Ti/O bond in TiO_2 , respectively^[19]. And the other two weak peaks of 459.8 and 453.9 eV are assigned to the state of TiH_2 . In the XPS spectra of V 2p (Fig.5d), two sub-peaks located at 156.4 eV and 158.4 eV were observed, which

hydrogenated plates.

The formed hydride particles produced brittleness of the Nb-Ti alloy, and the alloy was pulverized in argon atmosphere. Fig.7 shows the SEM images and the corresponding particle size distribution of the dehydrogenated powders crushed for varied periods of time. It is shown in Fig.7a that the powder crushed for 3 min is irregular polygon. The powder exhibits a wide particle size distribution, and the average particle size is approximately 36 μm . Most of the large particles with particles size of 50~100 μm remains, and a small amount of fine particles are formed. After milled for 5 min, the finer particles are mixed with a small number of coarse particles with particle size 40~60 μm . The

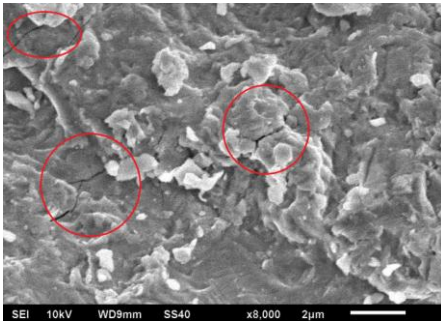


Fig.6 SEM image of the hydrogenated plates

powder crushed for 7 min exhibits normal distribution. A narrow particle size distribution is achieved. The size of the majority of the Nb-based particles is smaller than 9 μm together with small volume fraction of large particles. The powder exhibits similar irregular morphology to the mechanically alloyed powder, but the gains size is not as small

as that of the mechanically alloyed powder (14 nm) [22].

2.3 Dehydrogenating

Nb-Ti alloy hydrides was vacuum annealed in the temperature range of 100~800 $^{\circ}\text{C}$ to desorb hydrogen. Fig.8 shows the remained hydrogen and oxygen contents of the dehydrogenated powder with particle size smaller than 15 μm . The original hydrogen content of the powder is 1.14 wt%. At the dehydrogenation temperature of 100 $^{\circ}\text{C}$, the reduction of the hydrogen combined in the alloy is not obvious. When the temperature increases to 200 $^{\circ}\text{C}$, hydrogen content decreases sharply from 1.14 wt% to 0.15 wt%, suggesting that the combined hydrogen in the alloy can be easily destroyed. When the dehydrogenation temperature is higher than 400 $^{\circ}\text{C}$, minor change of hydrogen content is observed, and hydrogen content remains at the low level of around 0.001 wt%. Oxygen content of the dehydrogenated powder increases with the increasing dehydrogenation temperature due to the high reactivity of the alloying elements (such as Nb, Ti, Al, V) with oxygen and the high specific area of the powder. Oxygen contamination is at-

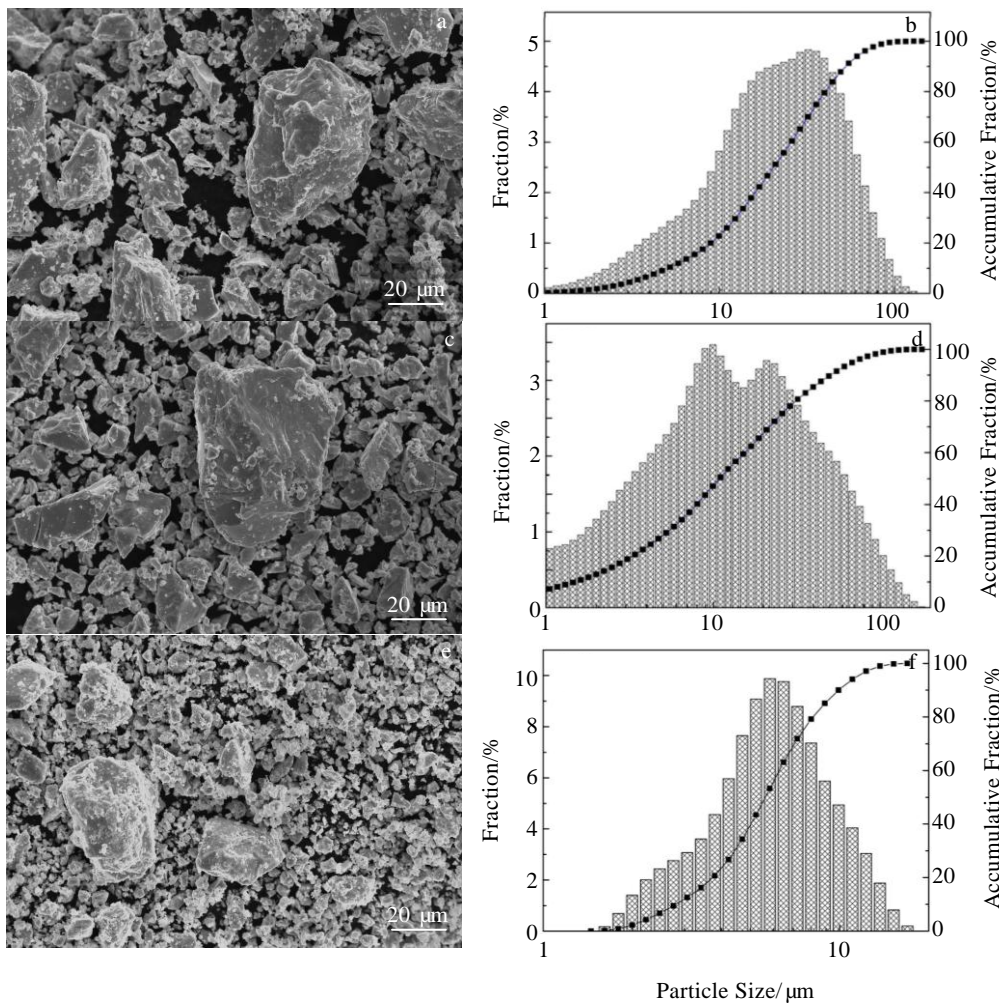


Fig.7 SEM images (a, c, e) and the corresponding particle size distribution (b, d, f) of the dehydrogenated powders crushed for varied periods of time: (a, b) 3 min (c, d) 5 min; (e, f) 7 min

tributed to the combination of highly activated surface in the hydrogenated and pulverized powder. In order to avoid excess contamination of the powder by oxygen impurity, dehydrogenating temperature of 400 °C is selected. The oxygen content of the powder after dehydrogenated at 400 °C is about 2980 $\mu\text{g/g}$

Fig.9 shows DSC results of the hydrogenated powders. The hydride phase forms exothermically and is generally a self-sustaining reaction. A large exothermic peak was observed at around 340 °C on the DSC curve, corresponding to the dehydrogenating process of the hydrogenated powder. This is in agreement with the rapid desorption rate in the temperature range of 100~300 °C. The peak temperature is higher than that of the rapid dehydrogenating temperature range (100~300 °C) shown in Fig.8. This is ascribed to the varied dehydrogenating atmosphere. DSC was performed in Ar gas atmosphere while dehydrogenating was carried out in vacuum, indicating that vacuum accelerates the dehydrogenating process.

Investigation of dehydrogenation behavior of the powder is important in deciding dehydrogenation temperature. Fig. 10 displays the XRD patterns of the powder dehydrogenated at varied temperatures. At the dehydrogenation tem-

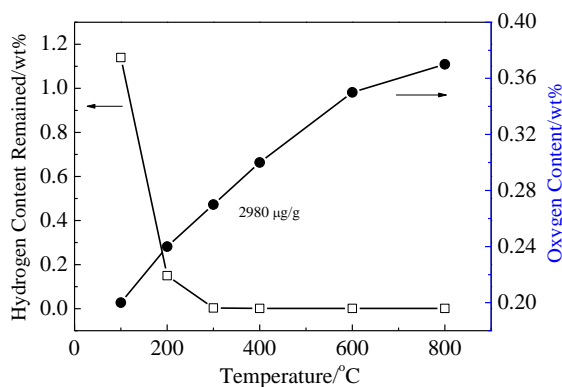


Fig.8 Remained hydrogen and oxygen contents of the dehydrogenated powder

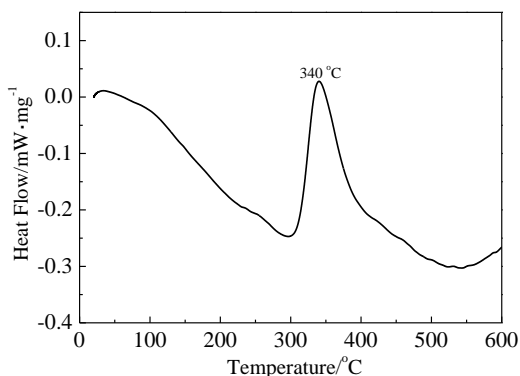


Fig.9 DSC curve of the hydrogenated powders

perature of 100 °C, less hydrogen is removed and phase constituent of the dehydrogenated remains unchanged compared with the hydrogenated powder ($\text{Nb}_{0.696}\text{V}_{0.304}\text{H}$). With the increase in dehydrogenation temperature, hydrogen is removed gradually, and phase constituent of the alloy changes correspondingly. At 200 °C, phase transformation from $\text{Nb}_{0.803}\text{V}_{0.197}\text{H}$ and TiH_2 hydrides to Nb-based solid solution (β phase) is observed. Additionally, the intensity of β peaks increases with the increasing dehydrogenation temperature. Therefore, the phase changes from Nb based solid solution (β phase) of the ingot to hydrides of Nb, V and hydrides of Ti during hydrogenation, and then back to its β phase after dehydrogenated. The peaks of $\text{Nb}_{0.696}\text{V}_{0.304}\text{H}$ vanish at 200 °C. The onset of dehydriding occurs at the temperature as low as 200 °C, suggesting the lower thermal stability of the hydrides. This phase transition temperature is lower than that of the niobium hydride (380 °C), which is associated with the interstitially dissolved alloying elements that enhances the equilibrium vacancy concentration and destabilizes the hydrides [16, 23]. Additionally, mild deformation during pulverization also accelerates hydrogen desorption. The absence of a peak position shift for the (111) β -phase reflection indicates that there is no significant variation of the lattice parameter of this phase during dehydriding, indicating that a possible decrease in lattice parameter due to hydrogen release could be compensated by thermal expansion effects. This result is in agreement with the result reported by Ref.[22].

Fig.11 shows XPS spectrum of the dehydrogenated powder. It reveals that the main compounds on the powder surface are TiO_2 and Nb_2O_5 , and the substrate is the Nb-based solid solution. Some Ti and Nb are found on the surface of the dehydrogenated powder. It is considered that, the hydrides of Ti and Nb decomposed and the Ti and Nb on the surface are hard to dissolve again into the substrate and the Ti and Nb inside dissolve again into the substrate to form the Nb-based solution phase.

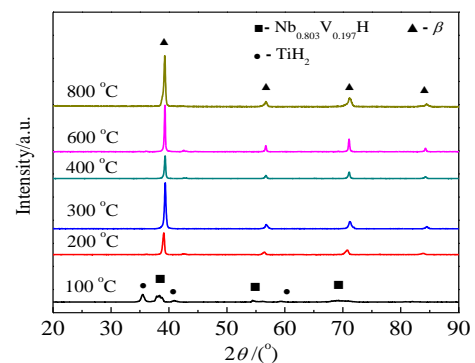


Fig.10 XRD patterns of the powder dehydrogenated at varied temperatures

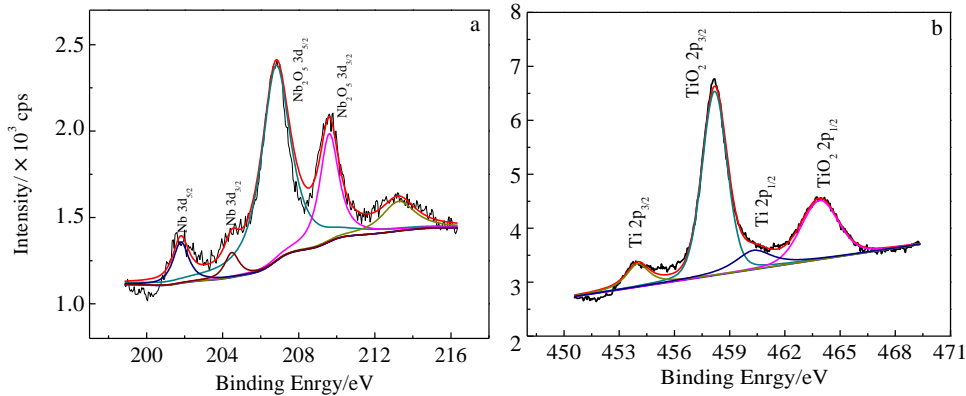


Fig.11 XPS spectra of the dehydrogenated powder: (a) Nb 3d and (b) Ti 2p

3 Conclusions

1) The Nb-Ti based alloy prepared by the hydride-dehydride process exhibits relatively low hydrogenation temperature and solid solubility limit of hydrogen. Hydrogen-induced binary and ternary hydrides ($\text{Nb}_{0.803}\text{V}_{0.197}\text{H}$, $\text{Nb}_{0.696}\text{V}_{0.304}\text{H}$ and TiH_x) are formed. The absorbed hydrogen is 1.12 wt% at the temperature of 400 °C.

2) Dehydrogenation of niobium and titanium hydride particles starts and completes at a relatively low temperature, and the remained hydrogen content is 0.001 wt% at 400 °C. After dehydrogenation, phase constituents of the powder change back to its original constituents (β phase).

3) Micro-fine light Nb based alloy powder with particle size below 10 μm is obtained. The oxygen content of the powders after dehydrogenated at 400 °C is about 2980 $\mu\text{g/g}$. The oxides on surface of the hydrogenated and dehydrogenated powder exist in the form of Nb_2O_5 and TiO_2 .

4) The hydride-dehydride process is approved to be an effective method to prepare Nb-Ti based alloy powder.

References

- Shi Z W, Wei H, Zhang H Y et al. *Materials Science & Engineering A*[J], 2016, 651: 869
- Zheng J S, Hou X M, Wang X B et al. *International Journal of Refractory Metals & Hard Materials*[J], 2016, 54: 322
- Shi Z W, Wei H, Zhang H Y et al. *Acta Materialia*[J], 2016, 105: 114
- Loria E A. *Materials Science & Engineering A*[J], 1999, 271(1): 430
- Tsukahara M, Takahashi K, Mishima T et al. *Journal of Alloys & Compounds*[J], 1996, 236(1-2): 151
- Gabriel S B, Brum M C, Candioto K C G et al. *International Journal of Refractory Metals & Hard Materials*[J], 2012, 30(1): 38
- Ding R, Jones I P, Jiao H. *Materials Science & Engineering A*[J], 2007, 458(1-2): 126
- Davidson D L, Chan K S. *Metallurgical & Materials Transactions A*[J], 2002, 33(2): 401
- Loria E A. *JOM*[J], 1987, 39(7): 22
- Zhang L T, Ito K, Vasudevan V K et al. *Acta Materialia*[J], 2001, 49(5): 751
- Ito K, Zhang L T, Vasudevan V K et al. *Acta Materialia*[J], 2001, 49(6): 963
- Zhang L T, Ito K, Vasudevan V K et al. *Intermetallics*[J], 2001, 9(12): 1045
- Zhang L K, Ito K, Inui H et al. *Acta Materialia*[J], 2003, 51(3): 781
- Patselov A M, Rybin V V, Greenberg B A et al. *Journal of Alloys & Compounds*[J], 2010, 505(1): 183
- Oh J M, Roh K M, Lee B K et al. *Journal of Alloys & Compounds*[J], 2014, 593(4): 61
- Barbis D P, Gasior R M, Walker G P et al. *Titanium Powders from the Hydride-dehydride Process*[M]. Oxford: Butterworth-Heinemann, 2015
- Oh J M, Lee B K, Suh C Y et al. *Materials Transactions*[J], 2012, 53(6): 1075
- Oh J M, Heo K H, Kim W B et al. *Materials Transactions*[J], 2013, 54(1): 119
- Ren N, Wang G, Liu H et al. *Materials Research Bulletin*[J], 2014, 50(2): 379
- Takeshita T. *Journal of Alloys & Compounds*[J], 1995, 231(1-2): 51
- Senkov O N, Chakoumakos B C, Jonas J J et al. *Materials Research Bulletin*[J], 2001, 36(7-8): 1431
- Zhang D Z, Qin M L, Din R et al. *International Journal of Refractory Metals & Hard Materials*[J], 2012, 32(7): 45
- Mitkov M, Boz'ic D. *Materials Characterization*[J], 1996, 37(2-3): 53

氢化脱氢法制备 Nb-Ti 基合金粉末

李启军^{1,2}, 章林¹, 李兵兵¹, 魏东斌¹, 曲选辉¹

(1. 北京科技大学 新材料技术研究院 北京材料基因工程高精尖创新中心 现代交通金属材料与加工技术北京实验室, 北京 100083)

(2. 航天材料及工艺研究所, 北京 100076)

摘要: 采用氢化-脱氢法制备了微细轻质 Nb-Ti 基合金粉末, 并研究了吸氢/解吸行为。300 °C 时, 氢吸收明显, 400 °C 时吸氢量达到饱和值 1.12% (质量分数)。氢化后形成二元和三元氢化物($\text{Nb}_{0.803}\text{V}_{0.197}\text{H}$, $\text{Nb}_{0.696}\text{V}_{0.304}\text{H}$, TiH_x)。由于氢致脆化效应, 吸氢后的粉末破碎后得到细粒径的氢化粉末。在脱氢过程中, 氢含量在 300 °C 时有效降低至 0.001%, 实现了从铌或钛氢化物到单相固溶体合金 (β 相) 的相转变。由于组分元素与氧反应活性高, 粉末中氧含量随吸氢或脱氢温度的升高而增加。为了防止杂质氧的污染, 氢化和脱氢温度都选择为 400 °C。实验最终得到了主要粒径小于 10 μm , 氧含量为 2980 $\mu\text{g/g}$ 的微细 Nb 基合金粉末, 且粉末表面的氧杂质主要以 Nb_2O_5 和 TiO_2 的形式存在。

关键词: 粉末冶金; Nb-Ti 基合金; 粉末制备; 氢化; 脱氢

作者简介: 李启军, 男, 1976 年生, 博士, 高级工程师, 北京科技大学新材料技术研究院, 北京材料基因工程高精尖创新中心, 北京 100083, E-mail: sichuanli@aliyun.com